The 2009 IEEE/RSJ International Conference on
Intelligent Robots and Systems
October 11-15, 2009 St. Louis, USA

On the Feasibility and Suitability of MR and ER Based Actuators in Human Friendly Manipulators

Alex S. Shafer, Mehrdad R. Kermani

***Abstract*—For several decades now, the robotics industry has postulated the emergence of a new breed of manipulators capable of safely interacting with humans. The integration of robots into human environments has always possessed a unique set of challenges. The primary concern has always been for the safety of the human coworkers. Insuring their safety has led to the desire to design manipulators with intrinsic safety characteristics. Specifically, it is noted that modern 'human-safe' manipulators are successful if they have minimized both their weight and reflected actuator inertia. The leading research accomplishing this relies on complex actuation systems. Such systems commonly suffer from degraded performance and high cost of development. Magneto- and Electro-Rheological fluids are a class of smart-materials that can instantaneously, and reversibly alter their rheological properties under the influence of an applied field. Devices developed with such fluids are known to possess superior torque-to-inertia characteristics over conventional servo systems. Moreover, their simple mechanical construction suggests that manipulators using such devices could be developed at a lower cost. In this paper, we will discuss the potential benefits rheological fluids can bring to the field of human friendly manipulators.**

I. Introduction

Increasingly, we are witnessing a growing number of developments in the field of robotics characterized by their intent to integrate man and machine in a safe and functional manner. The suitability of a manipulator to work in close proximity with humans is determined first by the level of safety it can guarantee towards its human counterparts. Much focus has been centered on interactive robots which are expected to perform in a safe and dependable manner in unknown and unpredictable environments. Arguably, the chief safety concern is the manipulator's response to collisions with humans. As we move closer and closer towards a shared environment between robots and humans, new approaches to manipulator design are becoming increasingly important.

Devices utilizing the unique properties of Magneto-Rheological (MR) and Electro-Rheological (ER) fluids have been developed for robotic applications, however almost entirely for use in haptic systems. While it has been suggested in the literature how such devices might be used in a manipulator to improve both safety and performance, there appears to be a general reluctance towards adopting such technology as a viable alternative to the current solutions.

In this paper, we will briefly discuss intrinsic properties of manipulators which have an impact on safety, as well as review some of the more notable actuation techniques and manipulator designs developed for human-safe manipulation. The unique properties of MR and ER fluids and how they can be leveraged to develop high performance, 'intrinsically safe' actuators are discussed next.

II. Human-Friendly Manipulators: Background and Analysis

In attempts to guarantee the safety of humans within a shared workspace, much research has been focused on the development of manipulators which are intrinsically safe. That is, manipulators which by means of their mechanical properties can guarantee some level of collision safety in the absence of a controller. To understand the degree of safety one might associate with a manipulator, we may look at the results of an uncontrolled collision through the use of the Head Injury Criterion (HIC) [1]. The HIC along with its variations have long been used by the automotive industry to gauge the severity of collisions. In the field of robotics, it can also be used to gain similar insight. The HIC is defined as

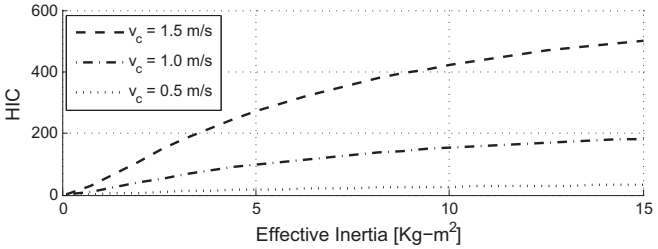

Fig. 1. Simulated HIC of a single axis manipulator

$$\text{HIC} = \max_{t_1,t_2}\left\{(t_2-t_1)\left(\frac{1}{t_2-t_1}\int_{t_1}^{t_2} a(t)dt\right)^{2.5}\right\} \quad (1)$$

where a is the acceleration of the head (in g's), and t_1 and t_2 are times within the collision selected to maximize the HIC, such that $t_1 < t_2$. An HIC of 100 is the maximum value considered to be non-life threatening. To gauge how the effective inertia of a link is related to a manipulator's inherent ability to collide safely, we simulate a single axis robot colliding with a human head (Fig. 1).

As we may have expected, the results of the HIC obviate that a manipulator's safety can be improved by reducing its effective inertia. Thus, was inspired the generation of light weight robots. One of the first manipulators to be designed under the light-weight paradigm was the Whole Arm Manipulator (WAM) [2]. The WAM uses steel cable transmission allowing actuators to be located at the manipulator's base. Another successful implementation is the the DLR-III [3]. Using light weight carbon composites to form its links, as well as advanced actuator design integrated with low weight harmonic reduction gears allows the DLR-III to attain a fully integrated light weight design. These approaches however addresses only half of the problem. Robotic manipulators make use of high performance servo motors to drive their links. These servo motors produce low output torque, and at high velocity with respect to what is suitable for most robots. To remedy this, gear reduction systems are most commonly employed. The resulting torque at the link is the actuator torque multiplied by the gear ratio G_r, while the reflected actuator inertia associated with the rotor of the motor is multiplied by ${G_r}^2$. Thus, the effective inertia experienced by

a robotic link can be expressed as

$$J_e \quad = \quad J_\ell + G_r^2 J_r, \tag{2}$$

where J_ℓ is the inertia of the link, and J_r is the rotor inertia of the motor. The reflected actuator inertia of a manipulators can in fact be much larger than that of the link inertia [4], thereby contributing a larger share of the inertial load during collisions. In response to this, several novel actuation systems have been proposed which work to decouple the reflected actuator inertia from the link. Receiving considerable attention are actuation systems that introduce compliance into their transmission. Series Elastic Actuator (SEA) [5] accomplishes precisely this by integrating an elastic element between the motor and link. During collisions, the elastic element acts to distribute the kinetic energy associated with the reflected actuator inertia over a larger period of time, reducing the severity of collisions. Intuitively, lower coupling stiffness results in collisions producing lower HIC values. The addition of the elastic element however dramatically reduces the controllable bandwidth of the manipulator. We can remark that the integration of SEA devices thus establishes a trade-off between safety and performance parameterized by the coupling stiffness. The Variable Stiffness Actuator (VSA) [6] was developed to address the stringent safety-performance trade-off characterized by the SEA. The VSA, like the SEA incorporates an elastic element into its transmission. The VSA however can alter the stiffness of the transmission coupling during task execution. It can be observed from Fig. 1 that at lower velocities, collisions involving stiff manipulators may still occur safely (resulting in a low HIC). Thus, by dynamically varying the stiffness of the transmission such that it is compliant for high velocity motion, and stiff at low velocities, accelerative ability can be improved while maintaining safety. In [7] Chew et al. proposed the Series Damper Actuator (SDA) as a means of achieving force/torque control. The SDA is constructed by placing a rotary damper in series with the motor drive. Force/torque control is achieved by controlling the relative angular velocity between the motor drive and the damper output. Similar to the SEA, the SDA has inherent impact absorption properties which are attributed to the dissipative nature of the series damper. Similarly to the addition of an elastic element, the SDA reduces the actuator bandwidth for decreasing coupling viscosity. Again, a trade-off exists between safety and performance, in this case parameterized by the damping coefficient. (It should be noted that the authors of [7] suggest how MR fluids can be used to vary the damping coefficient). Using a damping element over an elastic element subsequently reduces the order of the system by one. This implies that the SDA is capable of achieving a larger force bandwidth over the SEA. Variable Impedance Actuation (VIA) [8] combines both variable elastic, and variable damping elements in the transmission. This approach is an extension of the VSA concept. By being able to vary both an elastic, and a damping element, it is possible to again recuperate performance during task execution, while guaranteeing the safety of humans. The VIA further requires additional actuators to vary coupling parameters.

Another notable variation on the SEA is the Distributed Macro-Mini Actuation approach (DM^2) [4]. Actuation of the joint is achieved by the coupling of a low frequency-high torque SEA with a high frequency-low torque servo. The high-frequency servo, directly coupled to the joint, is used to actuate the manipulator in a complimentary frequency space to that of the SEA. In this way, the effective controllable bandwidth of the manipulator is improved. The low torque-high frequency servo is selected such that its output inertia is minimized. Thus, safety is maintained while performance is improved.

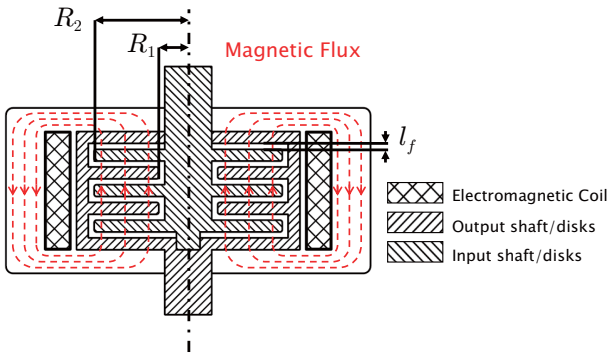

Fig. 2. Cross-section of a multi-disk style MR fluid clutch.

III. Fundamentals of MR and ER Fluid Based Actuators

and ER Fluids are a suspension of micrometer-sized particles in a carrier fluid. When subjected to an externally applied field - magnetic field for MR fluids, and electric field for ER fluids, the particles aggregate into columns aligning themselves in the direction of the applied field. Subsequently, the columns act to resist shearing of the fluid perpendicular to the field. The apparent yield stress of the fluid is dependant on, and increases with the intensity of the applied field. Using either MR or ER fluids, a clutch can be constructed such that the amount of torque it transmits can be controlled by the intensity of an applied field. Fig. 2 is a cross-section of a multi-disk style MR fluid clutch. The input shaft breaks out into a set of input disks which are aligned in parallel to a set of output disks attached to the output shaft. MR fluid fills the volume between input and output disks. Rotation of the input shaft causes shearing in the fluid with respect to the output shaft. By energizing the electromagnetic coil, a field is induced in the MR fluid altering its apparent viscosity. The outer casing of the MR clutch acts as the magnetic flux path required to complete the magnetic circuit. An ER clutch is formed much the same way, however does not require a magnetic coil. Applying high potential between input and output disks induces an electric field within the fluid. MR fluid clutches require ferromagnetic materials such as steel to form the magnetic circuit, while ER fluid clutches can make use of lighter materials such as aluminum.

A great deal of models have been developed to describe the behavior of both MR and ER fluids. The Bingham visco-plastic model is commonly used to represent the shear stress of the fluid as a function of the applied field, and shear rate. The model is given by

$$\tau \quad = \quad \tau_y(\mathbf{\Phi}) + \eta \frac{dv}{dz}, \; \tau > \tau_y \tag{3}$$

where τ is the shear stress, τ_y is the field dependant yield stress, $\mathbf{\Phi}$ is the applied field (magnetic field intensity $\mathbf{H}$ in MR device, and electric field $\mathbf{E}$ in ER device), η is the newtonian viscosity, and $\frac{dv}{dz}$ is the velocity gradient in the direction of the field. Applying the Bingham visco-plastic model to a clutch, we define r as the radius from the rotational axis, and l_f as the thickness of the fluid filled gap between input and output disks. In situations where $r >> l_f$ for

$r \in [R_1, R_2]$ (refer to Fig. 2), the velocity gradient becomes constant. We can then rewrite (3) as

$$\tau = \tau_y(\mathbf{\Phi}) + \eta\dot{\gamma}(r)\,,\ \tau > \tau_y \quad (4)$$

where the shear rate $\dot{\gamma}$ is defined as

$$\dot{\gamma} = \omega\, r\, {l_f}^{-1}, \quad (5)$$

and ω is the angular velocity between input and output shafts of the clutch. The torque produced by a circumferential element at a radius r is given by

$$dT = 2\pi r^2 \tau dr. \quad (6)$$

We define a clutch as having N output disks. Substituting (4) into (6) and integrating across both faces of each output disk, we arrive at

$$\begin{aligned} T &= 2N \int_{R_1}^{R_2} 2\pi\big(\tau_y(\mathbf{\Phi})r^2 + \eta\frac{\omega r^3}{l_f}\big)\, dr \\ &= 4N\pi\big(\frac{\tau_y(\mathbf{\Phi})({R_2}^3 - {R_1}^3)}{3} + \frac{\eta\omega({R_2}^4 - {R_1}^4)}{4l_f}\big) \end{aligned} \quad (7)$$

as the torque transmitted by an N-disk clutch. Data relating the yield stress τ_y of a fluid to an applied field are generally published by the manufacturer. The viscosity η of the carrier fluid is typically in the range of 0.1 to 0.3 Pa-s. The maximum torque transmission capability of an MR/ER clutch is dependent on the maximum yield stress the material can produce. MR fluids exhibit saturation in their yield stress at high field strengths. This is a result of the underlying physics, and limits the amount of torque a particular MR fluid can transmit in clutch applications. ER fluids on the other hand, experiences electrical breakdown at high field strengths, also limiting their torque transmission capacity. MR fluids can produce maximum yield stresses typically in the range of 50 to 100 kPa dependant on their chemistry. Alternatively, this value for ER fluids does not typically exceed 10 kPa. It should be noted that more recent research into the field of ER fluids has produced materials exhibiting a yield stress on par and even exceeding that of MR fluids [9].

Both MR and ER fluids respond to an applied field on the order of 1 ms. However, in the case of MR clutch, actuation response becomes delayed due to field propagation through the magnetic circuit [10]. As the magnetic field propagates from the coil, it is met by an opposing field produced by induction currents in the magnetic circuit. The response delay produced by this effect is exacerbated by the use of conductive material in the magnetic circuit. Special design techniques not unlike those used to construct large power transformers can be adopted to minimize the magnitude of the induced currents.

IV. Properties and Characteristics of MR and ER Fluid Based Actuators

Several configurations exist in which MR/ER clutches can be utilized to develop an actuation system. The simplest configuration utilizes a motor to drive either an MR or ER clutch, which in turn drives the joint. In this section, we will discuss some of the relevant properties of MR and ER clutches important for assessing their suitability as actuators. To generalize the discussion, we will consider simplified mechanical models of both clutch types. Note that in this section, we define the actuator output to be the output of either an MR or ER clutch.

A. Actuator Inertia

MR/ER actuators have the characteristic of replacing the reflected rotor inertia of the motor with the reflected inertia of the clutch output shaft and disks. The benefit of MR/ER actuators is their high torque to output moment of inertia ratio as compared to servo motors. To show this, we approximate the radius of the output shaft to be equivalent to R_1. The moment of inertia of a single output disk, J_d is given by

$$J_d = \frac{1}{2}\pi\rho_d l_f \left(R_2^4 - R_1^4\right) \quad (8)$$

where ρ_d is the mass density of the disk material, l_f is the thickness of the disk (commonly between 0.5 to 1 mm), and R_1 and R_2 define the minor and major radii respectively, of the output disk. If we consider the torque transmitted solely by the field dependant yield stress of the MR/ER fluid, the torque transmission of a single disk is then given by,

$$T_d = \frac{4}{3}\pi\tau_y \left(R_2^3 - R_1^3\right) \quad (9)$$

Furthermore, if we consider R_1 to be small, that is $R_2 \gg R_1$, then the contribution of the shaft region to both (8), and (9) is also small. By allowing R_1 to equal zero, we can approximate the torque-inertia ratio of a single disk to be

$$\alpha = \frac{T_d}{J_d} = \frac{8}{3}\frac{\tau_y}{\rho_d l_d R_2} \quad (10)$$

As observed the ratio becomes less favorable as R_2 increases. This however is not the final measure that dictates the actuators suitability. To grasp the overall effects of increasing radius, and hence torque capacity, the reflected inertia at the joint should be consider. The reason for this is that as radius increases along with torque capacity, the gear ratio required to amplify the actuator's torque decreases. As the actuator inertia multiplies the square of the gear ratio to arrive at the reflected inertia at the joint, the analysis becomes important. The reflected inertia of the MR/ER clutch at the manipulator joint is given by

$$J_c' = \frac{1}{2}\pi\rho_d l_d N \left(R_2^4 - R_1^4\right) G_r^2 \quad (11)$$

where we have included N to multiply the inertia by the number of disks in the clutch. The gear ratio G_r is defined as

$$G_r = T_c'/T_c \quad (12)$$

where T_c' is the desired torque at the joint, and T_c is the output torque of the clutch. Rearranging (9) to show the outer radius R_2 as a function of the clutch output torque yields

$$R_2 = \big(\frac{3}{4}\frac{T_c}{\pi\tau_y N} + R_1^3\big)^{1/3} \quad (13)$$

We can then write the equation representing the reflected inertia of an MR/ER clutch at the manipulator joint as a function of the clutch torque.

$$J_c' = \frac{1}{2}\pi\rho_d l_d N\Big(\big(\frac{3}{4}\frac{T_c}{\pi\tau_y N} + R_1^3\big)^{4/3} - R_1^4\Big)\Big(\frac{T_c'}{T_c}\Big)^2 \quad (14)$$

Fig. 3 shows the values of reflected actuator inertia versus output torque for both MR and ER fluid clutches as well as equivalent values for commercially available low-inertia servo motors. It is evident that both MR and ER fluid clutches demonstrate superior output inertia characteristics

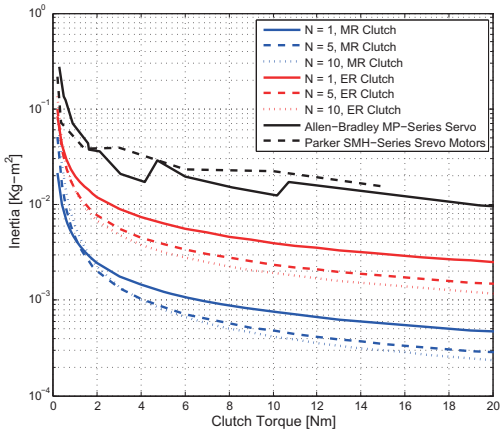

Fig. 3. Reflected inertia versus output torque for MR and ER fluid clutches ($T_c' = 50$ Nm, and parameters from Table I).

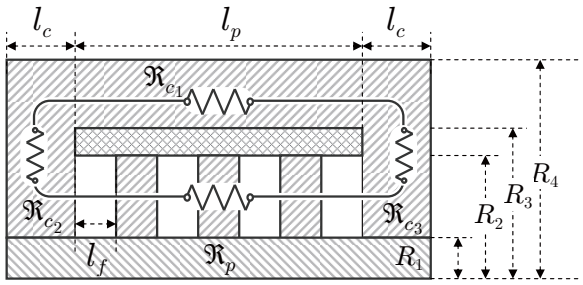

Fig. 4. Simplified MR clutch model: A single shaft extends the length of the clutch. Input and output disks have equivalent geometric and material properties. The electromagnetic coil is contained between R_2 and R_3, and R_4 defines the outer surface of the ferrous core.

over the low-inertia servo motors. We note that the developed inertia-torque relationship improves dramatically at larger values of output torque for both MR and ER fluid clutches.

B. Mass of Clutch

In this section we develop mass-torque relationships for MR and ER fluid clutches. While the relationships are developed using simplified geometric models, they serve to establish the order in which clutch mass compares to that of servo motors, as well as the rate at which the ratio evolves for increases torque capacity.

1) MR fluid clutch: To develop a relationship between clutch mass and torque capacity for MR fluid clutches, we consider the simplified geometric model detailed in Fig. 4. We will solve for required parametric values through the application of magnetic circuit analysis. We divide the reluctance of the core $\Re_c$ into three sections, namely $\Re_{c_1}$, $\Re_{c_2}$, and $\Re_{c_3}$. The symmetric geometry of the model dictates the reluctance $\Re_{c_2}$ to be equivalent to that of $\Re_{c_3}$. Thus we define the reluctance of the core to be

$$\Re_c \quad = \quad \Re_{c_1} + 2\,\Re_{c_{23}} \tag{15}$$

where $\Re_{c_{23}} = \Re_{c_2} = \Re_{c_3}$. We have defined a clutch by the number of output disks N coupled to the output shaft. For N output disks, a clutch is required to have $N-1$ input disks, and a total of $2N$ MR fluid interface gaps positioned between input and output disks. In the simplified model of Fig. 4, we define both geometric, and material properties of the input and output disks to be identical. The disk pack assembly thus contains $2N-1$ disks, and $2N$ MR fluid interface gaps. The reluctance of the disk pack assembly $\Re_p$ can then be written as

$$\Re_p \quad = \quad (2N-1)\,\Re_d + 2N\,\Re_f \tag{16}$$

where $\Re_d$, and $\Re_f$ are the reluctance of a single disk, and single MR fluid interface gap, respectively. The reluctance of a material is given by $\Re = l/(\mu_0\mu_r A)$, where l is the mean length of the flux path through the material, $\mu_0 = 4\pi \times 10^{-7}$ H/m is the permeability of free space, μ_r is the relative permeability of the material, and A is the cross sectional area of the material perpendicular to the flux path. Assuming the mean flux path through any of the circuit members lies at its geometric center, we can then derive the reluctance of the individual components of the simplified clutch model to be

$$\Re_{c_1} = \frac{l_p + l_c}{\mu_0\mu_{r_s}\,\pi\,(R_4^2 - R_3^2)} \tag{17}$$

$$\Re_{c_{23}} = \int_{\frac{R_2+R_1}{2}}^{\frac{R_4+R_3}{2}} \frac{dr}{\mu_0\mu_{r_s}\,(2\pi r)\,l_c} = \frac{\ln\left(\frac{R_4+R_3}{R_2+R_1}\right)}{2\mu_0\mu_{r_s}\,\pi l_c}$$

$$\Re_d = \frac{l_d}{\mu_0\mu_{r_s}\,\pi\,(R_2^2 - R_1^2)}, \quad \Re_f = \frac{l_f}{\mu_0\mu_{r_f}\,\pi\,(R_2^2 - R_1^2)}$$

Here, μ_{r_s} is the permeability of steel, the material used for both the core and disks, μ_{r_f} is the permeability of the MR fluid, W_d is the thickness of a single disk, l_f is the distance between input and output disks forming the MR fluid gap, l_c is the thickness of the equivalent core sections, and l_p is the length of the disk pack, given by

$$l_p \quad = \quad (2N-1)\,l_d + 2N l_f. \tag{18}$$

The flux in the circuit ϕ is then given by

$$\phi \quad = \quad I/(\Re_c + \Re_p) \tag{19}$$

where I is the total electric current through the cross section of the magnetic coil defined as,

$$I \quad = \quad l_p(R_3 - R_2)J_w \tag{20}$$

In (20), J_w is the current density of the coil cross section. The magnetic field intensity $\mathbf{H}$ at any point within the circuit is related to the circuit flux ϕ by

$$\mathbf{H} \quad = \quad \phi/(\mu_0\mu_r A) \tag{21}$$

where again, μ_r and A are respectively the relative permeability, and cross sectional area of the material at which the magnetic field intensity $\mathbf{H}$ is to be determined. We now define the parameter τ_y^* as the maximum yield stress at which the MR fluid is to operate. Using data provided by the MR fluid manufacturer [11] relating the yield stress of the fluid to the applied magnetic field, we define $\mathbf{H}^*$ as the magnetic field intensity in the MR fluid required to produce the yield stress τ_y^*. Rearranging (21), and substituting the appropriate MR fluid geometric and material values, we define ϕ^* as the flux required in the circuit to produce $\mathbf{H}^*$ in the MR fluid,

$$\phi^* \quad = \quad \mu_0\mu_{r_f}\,\pi\left(R_2^2 - R_1^2\right)\,\mathbf{H}^* \tag{22}$$

R_2 is uniquely defined by the parameters T_c, N, R_1 and τ_y^* (refer to (13)). Thus, for the given set of fixed parameters given in Table I, we solve for the values of R_3, R_4 and l_c

TABLE I
PARAMETER VALUES FOR SIMPLIFIED CLUTCH MODELS

MR Clutch Parameters			ER Clutch Parameters		
l_d	=	1×10^{-3} m	l_d	=	1×10^{-3} m
l_f	=	5×10^{-4} m	l_f	=	5×10^{-4} m
R_1	=	1×10^{-2} m	R_1	=	1×10^{-2} m
τ_y^*	=	39 kpa	l_c	=	7.5×10^{-3} m
J_w	=	2.5×10^6 A/m^2	R_4	=	$R_2 + l_c$
			τ_y	=	5 kpa

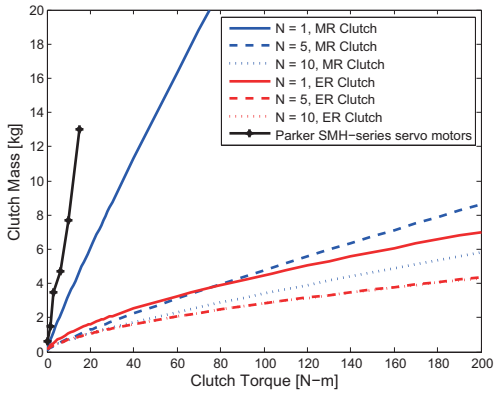

Fig. 5. Mass of simplified clutch models versus torque capacity

that satisfy (19) for $\phi = \phi^*$, while simultaneously minimizing the clutch mass m_{MRC}, given by

$$\begin{aligned} m_{\text{MRC}} &= m_c + m_p + m_s + m_w \\ m_c &= \pi \left[\left(R_4^2 - R_3^2\right) l_p + 2 \left(R_4^2 - R_1^2\right) l_c \right] \rho_s \\ m_p &= \pi \left[(2N-1)\, l_d \rho_s + 2N l_f \rho_f \right] \left(R_2^2 - R_1^2\right) \\ m_w &= \pi \left(R_3^2 - R_2^2\right) l_p \rho_{cu}, \quad m_s = \pi R_1^2 \left(l_p + 2\, l_c\right) \rho_{al}, \end{aligned} \tag{23}$$

where m_c is the mass of the core, m_p is the mass of the disk pack assembly which includes the MR fluid, m_s is the mass of the shaft, and m_w is the mass of the magnetic coil. In (23), ρ_s, ρ_f, ρ_{cu}, and ρ_{al} are respectively the mass densities of steel, MR fluid [11], copper, and aluminum. Fig. 5 shows the mass-torque relationship of the simplified MR clutch model and compares it to a commercially available servo motor. We note that due to the mass overhead associated with the material required to form the magnetic circuit, the mass-torque ratio of MR fluid clutches is less favorable at very low values N.

2) ER fluid clutch: The mass of an ER fluid clutch can be similarly approximated by again considering the simplified geometric model of Fig. 4. By assigning R_3 the value of R_2, the electromagnetic coil effectively vanishes from the model. We can then express the mass of an ER fluid clutch in terms of the mass equations previously developed, that is

$$m_{\text{ERC}} = m_p + m_s + m_c \tag{24}$$

however, we substitute the mass density of aluminum ρ_{al} for all components. As ER fluid clutches do not require ferromagnetic metals, there is more freedom to select lighter materials. Again, R_2 is defined by (13). Thus, given the values of the clutch parameters in Table I, we develop the mass-torque relationship for the simplified ER fluid clutch model reported in Fig. 5. In the developed mass-torque relationships of both MR and ER fluid clutches, we observe superior characteristics over the commercially available servo motor. More impressive is the fact that the mass-torque ratio remains consistent, or improves as the torque transmission capacity of the clutch is increased. Thus, even for very high torque requirements, such as those of Direct Drive (DD) systems, a low wight clutch solution becomes attractive.

V. DISTRIBUTED ACTIVE SEMI-ACTIVE ACTUATION

The Distributed Active Semi-Active (DASA) actuation configuration locates a driving motor (the active actuator) at the base of the robot, and a semi-active device (either an MR or ER fluid clutch) at the joint (refer to Fig. 6). The gear ratios G_1 and G_2 are balanced to give the desired mass, and reflected output inertia at the link. Reducing G_1 reduces the requirements of the clutch transmission torque which thus reduces the mass of the clutch, however the reflected output inertia is inevitably increased as G_2 must then be increased to compensate. In the previous sections have shown how actuating a joint via an MR or ER fluid clutch can be accomplished at greatly reduced mass and reflected output inertia versus conventional servo motors. The impact on safety is immediately appreciated as the effective inertia of the link is instantly reduced. This not only improves manipulator performance, but further allows a manipulator to operate at higher velocities while maintaining safe HIC values in the event of an collision. Moreover, the clutch itself is back driveable, and can be thought of as exhibiting the properties of an ideal torque source. The characteristic of back drivability has been identified as more than desirable in operations requiring physical interaction between man and machine. While motors themselves are also intrinsically back drivable, the high ratio gear reductions they require are often not. Thus, highly performing low weight robots which implement low mass motors at the expense of high ratio gear reductions rely on torque sensors in the control loop to electronically implement back-drivable behavior. MR and ER clutches have the added benefit of uniform torque transmission independent of armature position, unlike servo motors which suffer from nonlinearities such as cogging torque. Relocating the driving motor to the base of a robot in order to reduce the mass at the link is not a new concept. However, it has been a restrictive practice as the newly required transmission responsible for bringing mechanical power from the base to the joint has commonly introduced unwanted friction and compliance which have reduced performance, and complicated the control system. The DASA implementation however can be controlled to operate in a region in which torque transmission is relatively immune to perturbation in the relative angular velocity ω within the clutch. This characteristic allows the DASA system to function with less than ideal mechanical transmission while maintaining the performance and characteristics of a 'stiff' transmission at the joint. To explain this, we consider that the the Bingham model is accurate for describing the rheology of the fluid for shear stress τ above the field dependant yield stress τ_y as expressed in (3). It is this 'Bingham region' in which we wish the clutch to operate in order to benefit from the aforementioned characteristics. Below the yield stress τ_y however, the fluid exhibits newtonian characteristics, that is to say that τ grows with a non-negligible proportionality to the shear rate $\dot{\gamma}$. (For a more in-depth analysis into rheological modeling of MR fluids and the source for this discussion, see [12]). We can thus attribute a field dependant shear rate threshold $\dot{\gamma}^*$ below which the fluid exhibits newtonian characteristics, and above which, the Bingham model applies. To maintain the clutch in the Bingham region, the fluid at any radius r within the clutch must maintain a shear rate $\dot{\gamma}$ above

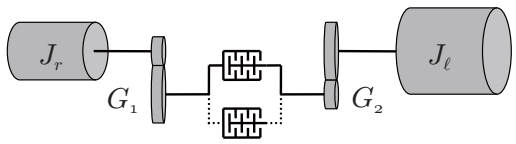

Fig. 6. Distributed Active Semi-Active Actuation: Solid line represents single clutch configuration, dotted line represents connection to second clutch present only in antagonistic configuration.

$\dot{\gamma}^*$. To guarantee this condition, we define the field dependant angular velocity ω^*, the threshold above which operation in the Bingham region is ensured as

$$\omega^* \quad = \quad \dot{\gamma}^* l_f {R_1}^{-1}. \tag{25}$$

We come to (25) by rearranging (5) and substituting r with its minimum value R_1. R_1 must be used as it is the critical radius at which the lowest shear rate $\dot{\gamma}$ occurs within the clutch. The control strategy should therefore attempt to avoid entering the newtonian region by controlling the motor angular velocity ω_m to satisfy the condition

$$|\omega_m| \quad = \quad |\omega_j - \omega^*| + \epsilon^* \tag{26}$$

where ω_j is the angular velocity of the joint, and ϵ^* is a field dependant error margin selected to ensure that the dynamics of the motor have enough time to react to quickly varying values of ω_j. ϵ^* must be large enough to ensure $\omega \geq \omega^*$ under all dynamic situations, however exact calculation of ϵ^* may be difficult as there is a reliance on empirical data associated with the dynamics of the joint/link. Care must be taken, however, to avoid unnecessary power dissipation, which for a clutch is defined as $P_d = T\omega$. Because ω tracks $\omega^* + \epsilon^*$, the value selected for ϵ^* cannot be arbitrarily large. Crossing into the newtonian region is required to alter the direction of the torque transmitted to the link when utilizing a single clutch to implement the DASA system. As the motor must change the direction of its output rotation, the clutch torque transmission momentarily enters a dead-zone (courtesy of the newtonian characteristics), the extent of time in which spent is dependant on the dynamic capabilities of the motor. This has the potential, and in fact probability of creating substantial backlash, which could severely handicap the system's ability to effectively accomplish precision position control.

VI. Antagonistic-DASA

An antagonistic configuration of the DASA system is intended to increase performance, and rectify the shortcomings of the single clutch DASA system discussed in the previous section. The transmission shaft drives the input to both clutches (Fig 6), however in opposite directions with respect to one another. The antagonistic output of the two clutches is coupled to the link. By energizing one of the two clutches, torque can be transmitted in either the clockwise, or counterclockwise direction. Thus, the antagonistic configuration allows for torque transmission to the joint to alter direction without altering the direction of the motor output, thereby eliminating the backlash introduced by the single clutch DASA. Such devices have been developed for ER fluids. Sakaguchi and Furusho developed a Two-Directional-Rotational-Type ER Actuator having very high performance characteristics [13]. Maintaining rotation of the motor shaft, the bandwidth of the antagonistic-DASA output is limited by charging, and discharging of the relevant field required to activate the clutch pair. It is anticipated that an antagonistic DASA implementation utilizing ER clutches will have a higher controllable bandwidth over an MR DASA equivalent. This is due to the short charge time associated with electric fields as compared to the propagation of the magnetic field through the magnetic circuit of an MR clutch. If we label the two clutches of an Antagonistic DASA assembly as $\mathcal{C}_1$, and $\mathcal{C}_2$, then the motor's angular velocity should track

$$\omega_m \quad = \quad \max\{|\omega_j - \omega_1^*|, |\omega_2^* - \omega_j|\} + \epsilon^* \tag{27}$$

to avoid entering the Newtonian region of operation in either clutch. ω_1^*, and ω_2^* are the angular velocity of the Bingham region thresholds for clutches $\mathcal{C}_1$, and $\mathcal{C}_2$ respectively. Note that in our convention, clutch $\mathcal{C}_2$ has its input reversed in direction with respect to clutch $\mathcal{C}_1$, that is $\omega_1 = \omega_j - \omega_m$, while $\omega_2 = \omega_j + \omega_m$.

VII. Conclusion

MR and ER fluids exhibit promising characteristics for applications in robotics. Specifically, they are well suited for actuation systems developed to interact physically with humans. As we have shown, MR and ER clutch based actuators demonstrate excellent mass-torque, and inertia-torque ratios. This is especially evident for clutches having large torque capacities. This creates a niche opportunity for MR and ER based actuators to be developed into light-weight Direct-Drive (DD) systems. Light-weight DD systems exhibit several characteristics which are very much sought after for human friendly manipulators. Namely: intrinsic back-drivability, low output inertia, superior performance and bandwidth, and precision controllability of output torque.

References

[1] J. Versace, "A review of the severity index," *Proc. of* 15^{th} *Stapp Car Crash Conf.*, pp. 771–796, 1971.

[2] K. Salisbury, W. Townsend, B. Ebrman, and D. DiPietro, "Preliminary design of a whole-arm manipulation system (wams)," in *Proc. IEEE Int. Conf. on Rob. Autom.*, 1988, pp. 254–260.

[3] G. Hirzinger, J. Bals, M. Otter, and S. J., "The DLR-Kuka success story: robotics research improves industrial robots," *IEEE Rob. Autom. Mag.*, vol. 12, no. 3, pp. 16–23, 2005.

[4] M. Zinn, O. Khatib, and B. Roth, "A new actuation approach for human friendly robot design," in *Proc. IEEE Int. Conf. on Rob. Autom.*, 2004, pp. 249–254.

[5] G. Pratt and M. Williamson, "Series elastic actuators," in *Proc. IEEE/RSJ Int. Conf. on Intell. Rob. Syst.*, 1995, pp. 399–406.

[6] G. Tonietti, R. Schiavi, and A. Bicchi, "Design and control of a variable stiffness actuator for safe and fast physical human/robot interaction," in *Proc. IEEE Int. Conf. on Rob. Autom.*, 2005, pp. 526–531.

[7] C.-M. Chew, G.-S. Hong, and W. Zhou, "Series damper actuator: a novel force/torque control actuator," in *Proc.* 4^{th} *IEEE/RAS Int. Conf. Humanoid Rob.*, vol. 2, 2004, pp. 533–546.

[8] A. Bicchi, G. Tonietti, and R. Schiavi, "Safe and fast actuators for machines interacting with humans," in *Proc.* 1^{st} *IEEE Tech. Exhib. Based Conf. on Rob. Autom. TExCRA '04*, 2004, pp. 17–18.

[9] W. Wen, X. Huang, S. Yang, K. Lu, and P. Sheng, "The giant electrorheological effect in suspensions of nanoparticles," *Nat. Mater.*, vol. 2, pp. 727–730, 2003.

[10] N. Takesue, J. Furusho, and Y. Kiyota, "Fast response MR-fluid actuator," *J. Soc. Mech. Eng. Int. J. Ser.C:*, vol. 47, no. 3, pp. 783–791, 2004.

[11] Lord Corporation, "MR-132DG Magneto-Rheological Fluid," Lord Tech. Data, July 2008, rev. 1. [Online]. Available: http://www.lordfulfillment.com/upload/DS7015.pdf

[12] R. S.-R. Daniela Susan-Resiga, Ladislau Vks, "A rheological model for magneto-rheological fluids," in 3^{rd} *Ger. Romanian Workshop on Turbomach. Hydrodyn.*, 2007.

[13] M. Sakaguchi and J. Furusho, "Development of high-performance actuators using er fluids," *J. Intell. Mater. Syst. Struct.*, vol. 10, No. 8, pp. 666–670, 1999.